

Abstract

Two-dimensional (2D) tetragonal group-V materials have attracted considerable interest, while their topological properties remain largely unexplored. Using density functional theory, topological quantum chemistry theory, and a tight-binding model, we show that monolayer tetragonal antimonene (T-Sb) realizes a higher-order topological insulator (HOTI). A layer-dependent analysis reveals an even-odd oscillation between HOTI and trivial phases with varying layer numbers. Upon stacking these 2D layers into a three-dimensional structure, successive phase transitions from a metal to a strong topological insulator and eventually to a weak HOTI are driven by tuning the interlayer van der Waals (vdW) coupling. Tight-binding (TB) model analysis shows that these transitions are closely related to the vdW-modulated vertical hopping strength and onsite energy of Sb p_z orbitals. Moreover, the TB model predicts a weak topological insulator phase within an appropriate parameter regime of interlayer vdW interaction and spin-orbit coupling, as verified in T-Sb materials. These results highlight vdW engineering as an experimentally accessible strategy for designing diverse topological phases based on 2D HOTIs.

Result1: Higher-order topology in monolayer T-Sb

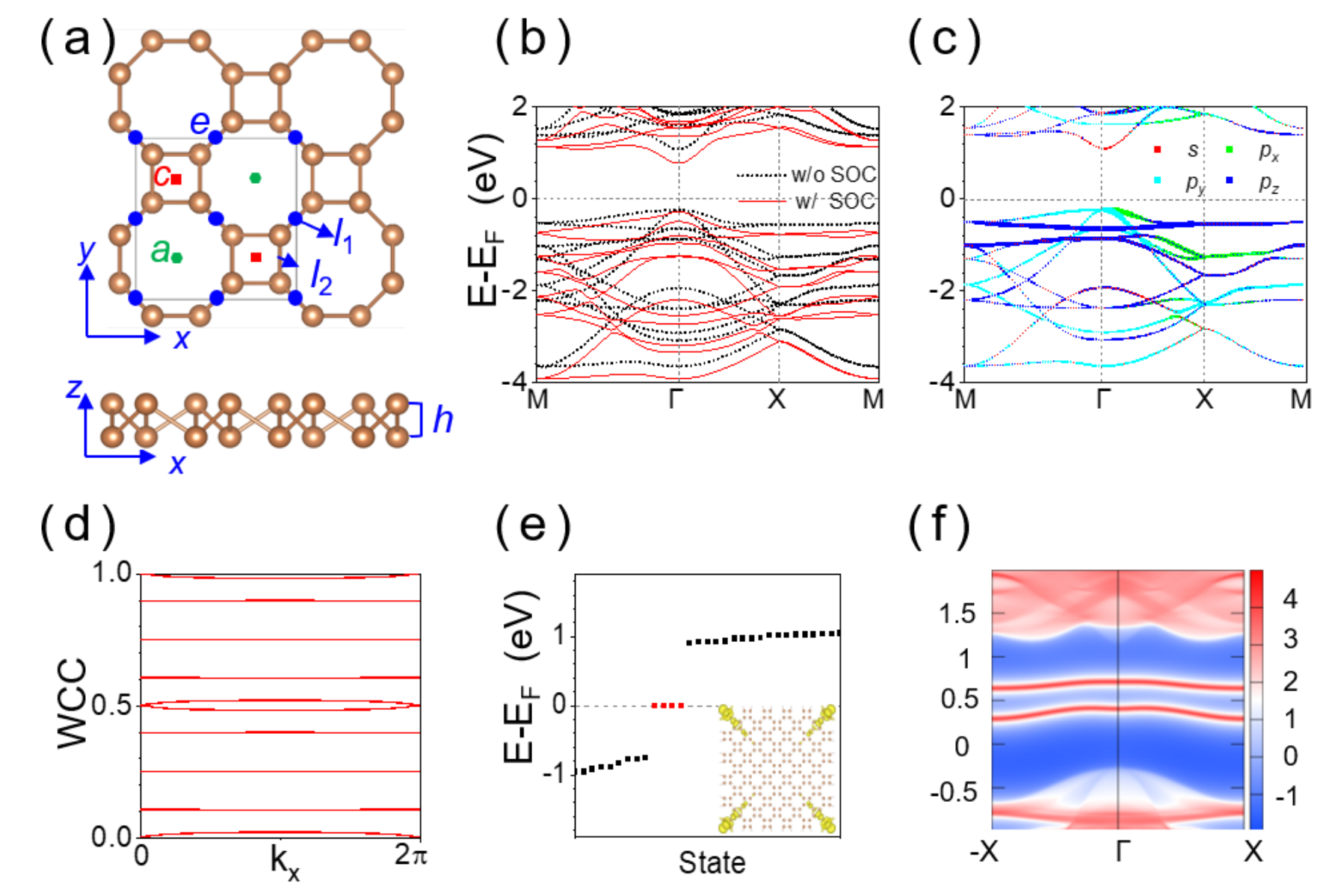


Fig. 1: (a) Top and side views of the T-Sb monolayer. The maximal Wyckoff positions (2a, 2c, and 4e) are also given. (b) Band structures of the 1L T-Sb. (c) Projected band structures of Sb s and p orbitals in the 1L T-Sb without SOC. (d) Evolution of the Wannier charge centers of 1L T-Sb without SOC. (e) Energy levels of a finite 1L T-Sb flake calculated by using DFT, where red dots denote corner states. The bottom-right inset shows the distribution of the corner states in the T-Sb flake. (f) Edge states of a semi-infinite 1L T-Sb without SOC.

Result2: Even-odd oscillation behavior in few-layer T-Sb

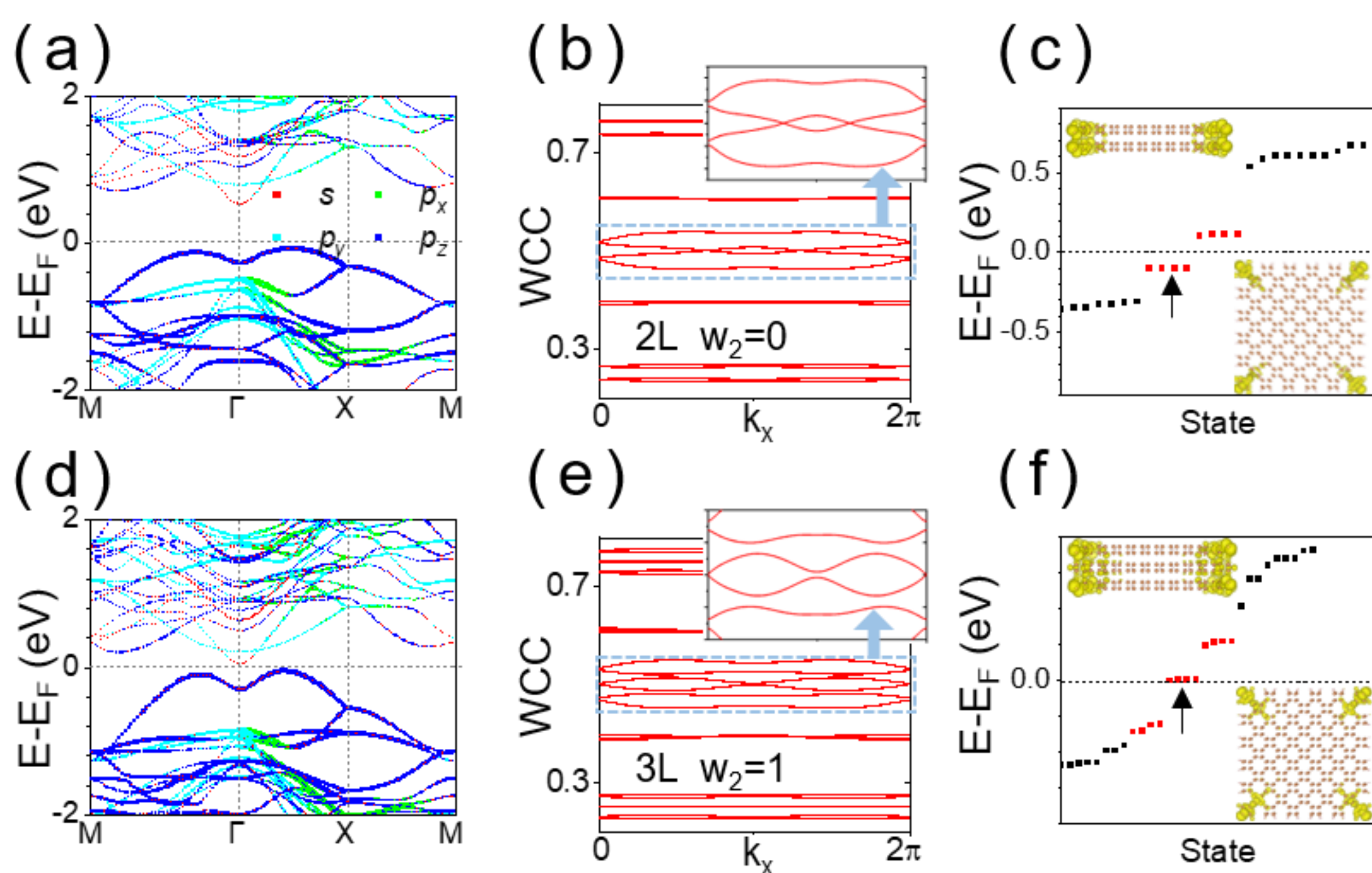


Fig. 2: (a) Projected band structures of the 2L T-Sb without SOC. (b) Evolution of the WCCs in the 2L T-Sb. The inset shows an enlarged view of the region marked by the blue dashed rectangle. (c) Energy levels of a 2L T-Sb flake calculated by using DFT. The black arrow marks the occupied corner states. The two insets illustrate the side and top views of the corner states in the 2L T-Sb flake. (d-f) Same as (a-c), respectively, but for 3L T-Sb.

Result3: Diverse topological phases in 3D T-Sb

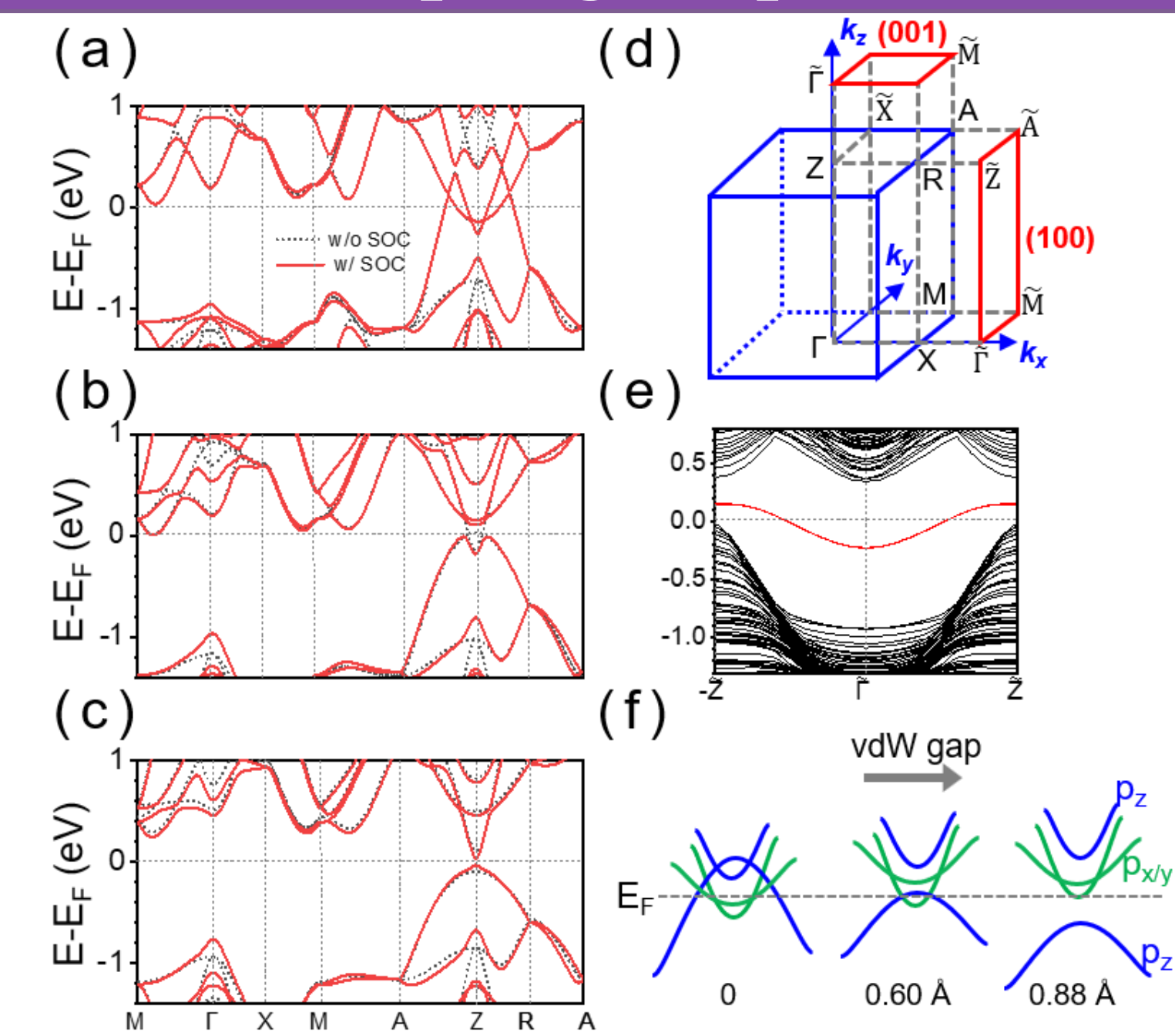


Fig. 3: (a-c) DFT-calculated band structures of 3D T-Sb with interlayer expansions along the z direction of $\Delta H = 0.0 \text{ \AA}$, 0.60 \AA , and 0.88 \AA , respectively. The SOC is not taken into account. (d) The 3D Brillouin zone with its projected (001) and (100) planes. (e) DFT-calculated hinge states: four degenerate states near E_F . (f) Schematic illustrating the shifting trend of $p_{x,y}$ and p_z orbitals with decreasing vdW coupling, based on DFT calculations.

Result4: Tight-binding model for 3D T-Sb

A 3D TB model involving the $p_{x,y}$ and p_z orbitals on each Sb atom is constructed to elucidate the mechanism responsible for the rich topological phases in the 3D T-Sb. The TB Hamiltonian is written as

$$H_{3D} = H_{\text{onsite}} + H_{\text{in}} + H_{\text{ver}} + H_{\text{soc}}$$

where H_{onsite} describes the orbital-dependent onsite energies,

$$H_{\text{onsite}} = \varepsilon_{p_{x/y}} \sum_i c_{p_{x/y}}^\dagger c_{p_{x/y}} + \varepsilon_{p_z} \sum_i c_{p_z}^\dagger c_{p_z}$$

In Eq. (6), c_{α}^\dagger (c_{α}) represents a creation (annihilation) operator for an electron with α ($\alpha = p_{x,y}$ and p_z) orbitals on site i . ε_{α} is the onsite energy for orbital α . The H_{in} term in Eq. (5) denotes the intralayer Hamiltonian,

$$H_{\text{in}} = \sum_{i \neq j} V_{ij} (c_i^\dagger c_j + h.c.),$$

where V_{ij} indicates the hopping integral between sites i and j within each layer.

According to the DFT band structure, the interlayer coupling is dominated by the p_z orbital, whereas the p_x and p_y orbitals contribute primarily to the intralayer interactions and are thus negligible for the interlayer hopping. Therefore, the H_{ver} term in Eq. (5), which describes the vertical interlayer hopping, is only considered for the p_z orbital:

$$H_{\text{ver}} = \sum_{\substack{i \in \{4,5,6,7\} \\ j^+ \in \{0,1,2,3\}}} J_z m_{p_z} c_i^\dagger c_{j^+} + \sum_{\substack{i \in \{0,1,2,3\} \\ j^- \in \{4,5,6,7\}}} J_z m_{p_z} c_i^\dagger c_{j^-} + h.c.,$$

where i labels the intralayer atomic sites within a given Sb layer, while j^+ and j^- denote the corresponding atomic sites in the adjacent upper and lower Sb layers, respectively. The J_z and $m_{i,j}$ indicate the interlayer interaction coefficient and hopping integral via the p_z orbitals, respectively. Only the nearest-neighbor hopping interactions are considered in the model. The H_{soc} term in Eq. (5) represents the onsite SOC term. Excellent agreement with the DFT band gap and dispersion is achieved by using three fitting parameters: J_z , ε_{p_z} , and λ , where λ denotes the SOC strength.

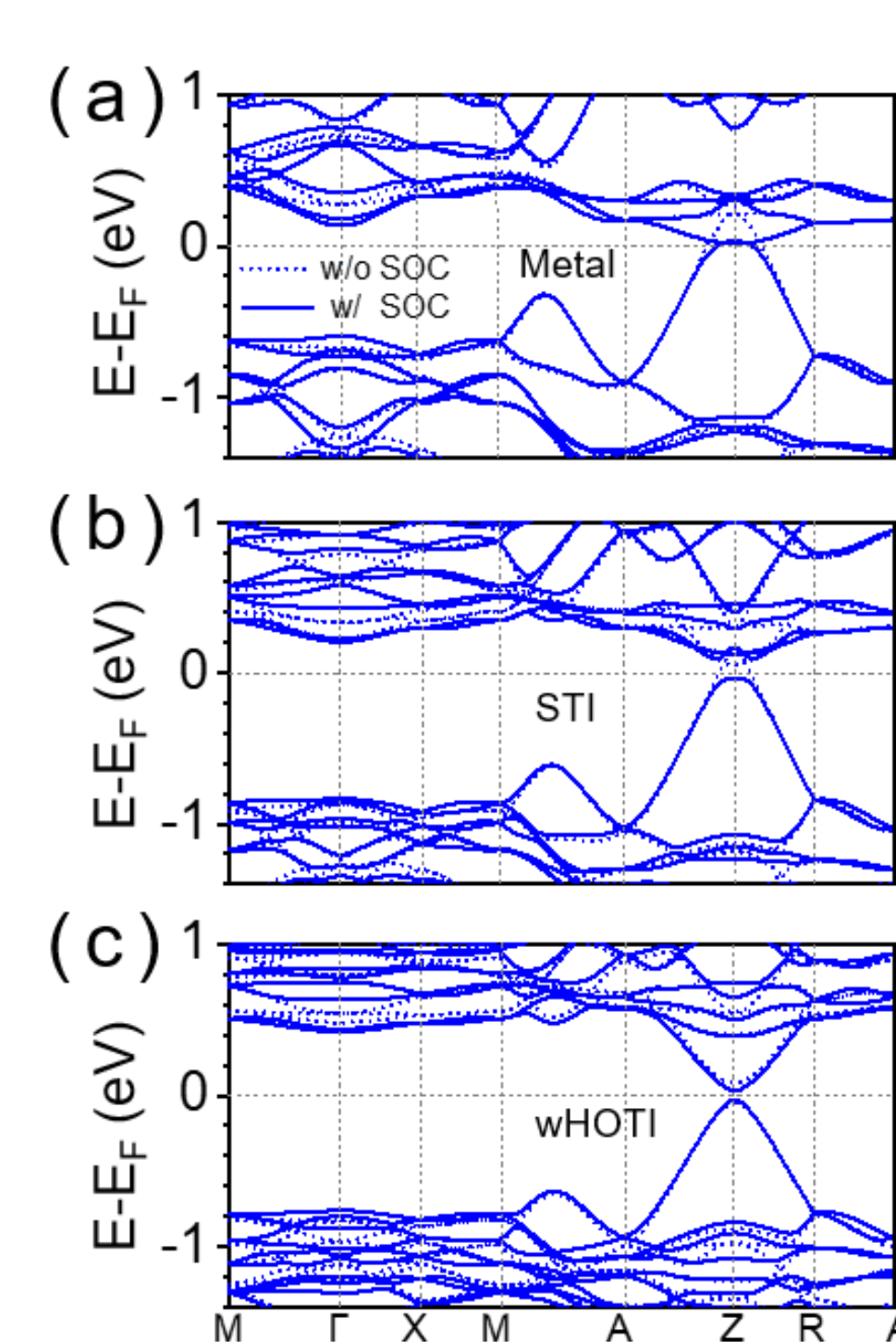


Fig. 4: Band structures of the TB model without SOC ($\lambda = 0 \text{ eV}$, dotted curves) and with SOC ($\lambda = 0.11 \text{ eV}$, solid curves). The parameters (in eV) are: (a) $J_z = 0.38$, $\varepsilon_{p_z} = 1.21$. (b) $J_z = 0.30$, $\varepsilon_{p_z} = 0.64$. (c) $J_z = 0.25$, $\varepsilon_{p_z} = 0.27$. Panels (a-c) correspond to metal, STI, and wHOTI phases, respectively. The trend is consistent with the DFT results shown in Figs. 3(a-c).

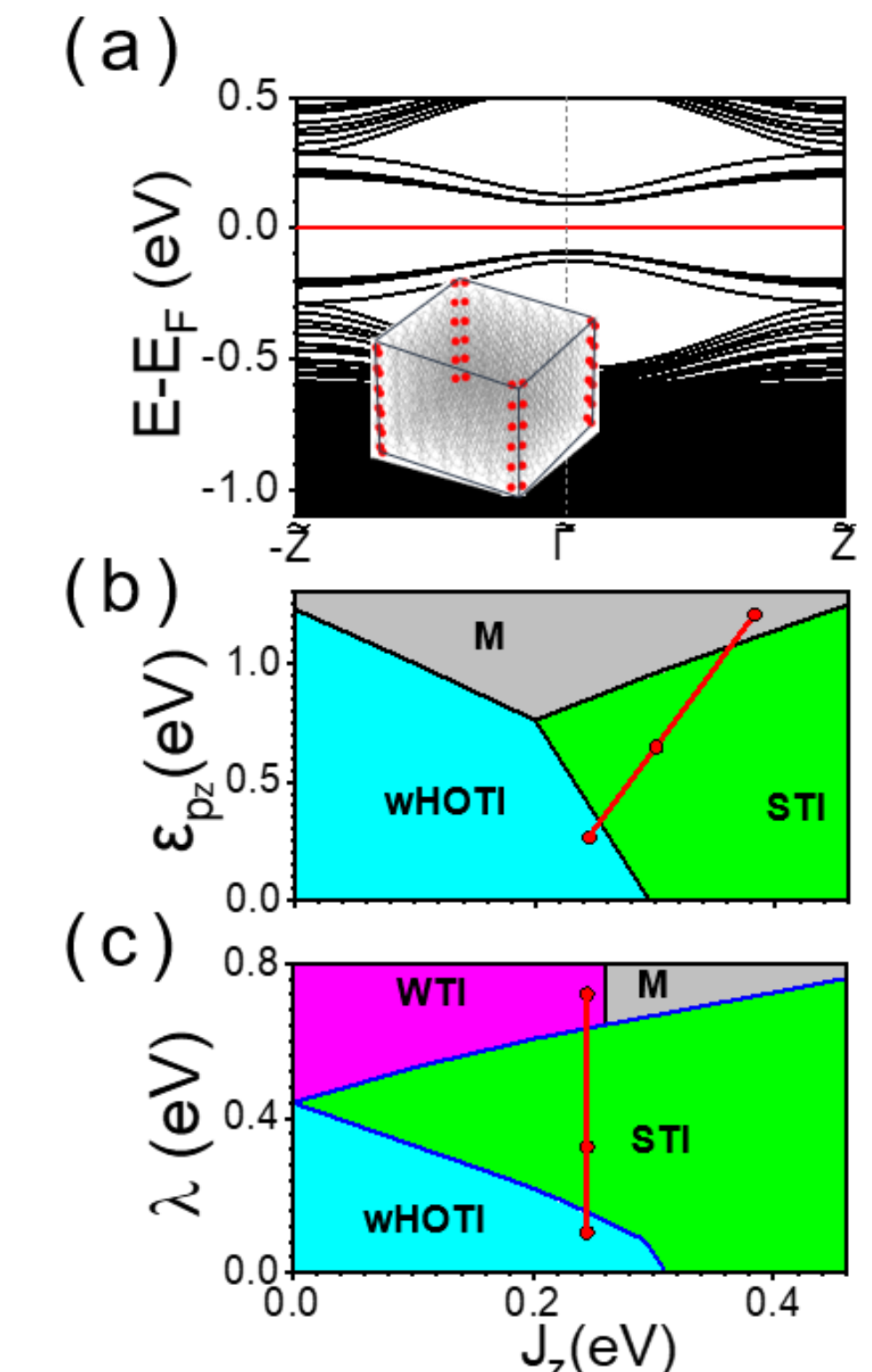


Fig. 5: (a) Hinge (red) and bulk (black) states from the TB model with parameters as in Fig. 5(c). The inset in (a) shows the hinge-state charge distribution. (b, c) Phase diagrams of 3D T-Sb from the TB model, showing the wHOTI (blue), STI (green), WTI (magenta), and metallic (gray) phases. In (b) and (c), the λ and ε_{p_z} are fixed at 0.11 eV and 0.27 eV , respectively. In (b), the three red points on the red line (from right to left) correspond to Figs. 5(a-c), respectively. In (c), the three red points on the red line (from bottom to top) correspond to Figs. S10(a, b, and d) in the SM^[45], respectively.

Conclusions

We demonstrate that monolayer group-V T-Sb is a higher-order topological insulator, characterized by corner states originating from a filling anomaly at the $4e$ Wyckoff position. Layer-dependent calculations reveal an even-odd oscillatory topological transition between HOTI and trivial insulating phases, with its oscillation period dictated by the denominator of the corner charge ($e/2$) in the monolayer limit. By engineering the stacking of 2D HOTI layers with tunable interlayer coupling, we realize various topological phases in 3D T-Sb, including STIs and wHOTIs. Notably, the metal-STI-wHOTI topological transitions in 3D T-Sb is quantitatively captured by the established TB model, arising from the reduced vdW interlayer hopping and onsite Sb p_z orbital energy. The interplay between the vdW interlayer coupling strength and the SOC can also give rise to rich topological phases. Intriguingly, a novel WTI phase predicted from the TB model is confirmed in 3D T-Sb by DFT calculations. Our work identifies T-Sb as a versatile functional platform for tailoring tunable topological phases and provides a practical design principle for engineering layered topological materials.

Contact

Wenting Xu
Zhongqin Yang's Group
Email: 24110190093@m.fudan.edu.cn
Phone: 17770353398

References

- [1] W. Xu, Y. Xue, Y. Zhu, W. Xu, and Z. Yang, Second-order topological insulator and its transition to quantum spin Hall state in a hydrogenated tetragonal stanene, *Phys. Rev. Mater.* **8**, 074001 (2024).
- [2] Y. Zhu, B. Zhao, Y. Xue, W. Xu, W. Xu, and Z. Yang, From Topological Nodal-Line Semimetals to Quantum Spin Hall Insulators in Tetragonal SnX Monolayers (X=F, Cl, Br, I), *Chin. Phys. Lett.* **41**, 067301 (2024).